

**\*\*FULL TITLE\*\***

*ASP Conference Series, Vol. \*\*VOLUME\*\*, \*\*YEAR OF PUBLICATION\*\**

**\*\*NAMES OF EDITORS\*\***

## Galactic Planetary Nebulae in the AKARI Far-Infrared Surveyor Bright Source Catalog

Nick Cox,<sup>1</sup> Arturo Manchado,<sup>2,3</sup> Pedro García-Lario,<sup>1</sup> Ryszard Szczerba<sup>4</sup>

<sup>1</sup> *Herschel Science Centre, European Space Astronomy Centre, European Space Agency, Spain*

<sup>2</sup> *Instituto Astrofísica de Canarias, Spain*

<sup>3</sup> *CSIC, Spain*

<sup>4</sup> *N. Copernicus Astronomical Center, Poland*

**Abstract.** We present the results of our preliminary study of all known Galactic PNe (included in the Kerber 2003 catalog) which are detected by the AKARI/FIS All-Sky Survey as identified in the AKARI/FIS Bright Source Catalog (BSC) Version  $\beta$ -1.

### 1. Introduction

Planetary Nebulae (PNe) are low-mass stars that have evolved along the evolutionary track from AGB, post-AGB, proto-PN to PN. One important goal of far-infrared (FIR) studies of PNe is to identify the FIR excess which provides important information on the mass loss history experienced by these stars in the recent past. We have performed a preliminary analysis of known Galactic PNe (taken from the Kerber et al. (2003) catalog) and their presence and properties in the  $\beta$ -1 release of the AKARI/FIS bright source catalog (BSC). We discuss potential technical issues related to the catalog and the effect on the study of PNe. Independent AKARI and IRAS spectral energy distributions (SEDs) are fitted with simple dust models to understand detection limits, calibration limitations and biases affecting the PN sample.

### 2. Galactic PNe in the BSC

About 40% of the known PNe (Kerber et al. 2003) are detected by AKARI/FIS while 63% can be identified in the IRAS point source catalog (PSC). This discrepancy is partly explained by gaps in sky-coverage of the AKARI/FIS BSC but also by differences in the point source flux sensitivity between these two surveys. Currently, there is not yet information available on the sky coverage (e.g. number of scans across a certain region of the sky). Noteworthy is the fact that AKARI/FIS detected a number of PNe that were not detected by IRAS.

#### 2.1. Flux Sensitivity and Completeness

From the initial set of PNe found in both IRAS and AKARI catalogs we selected only those with good quality flux values at 60 and 65  $\mu\text{m}$ , respectively. We

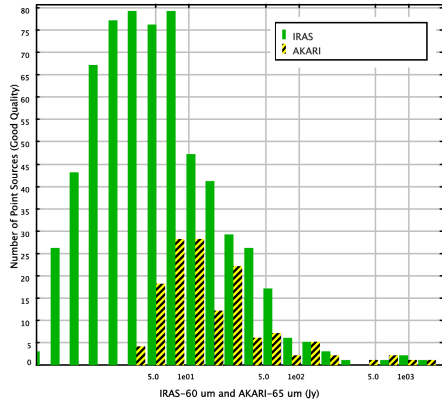


Figure 1. PNe detected by IRAS-60  $\mu\text{m}$  and AKARI-65  $\mu\text{m}$  bands.

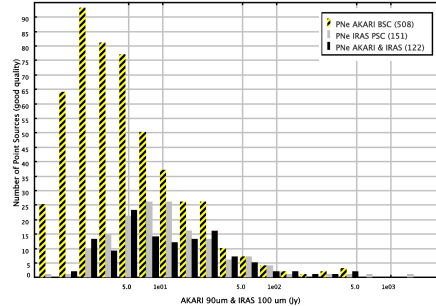


Figure 2. PNe detected by AKARI-90  $\mu\text{m}$ , IRAS-100  $\mu\text{m}$  bands, and both.

selected this band since the IRAS-100 fluxes are generally of worse quality though the AKARI-90 fluxes are better than the AKARI-65 fluxes (only 139 have good quality 65 flux; and 629 good IRAS-60). For the AKARI-65 band there are (almost) no reliable point sources with flux densities less than 4 Jy, whereas IRAS detected many PNe below the 1 Jy limit. This can be clearly seen from Figure 1 which shows the number of sources (of good quality) versus the IRAS and AKARI fluxes. The picture for the AKARI-90 and IRAS-100 fluxes is, however, the opposite. For this wavelength IRAS is severely limited (by presence of cirrus emission) whereas AKARI gives many good detections (also below 4 Jy). See Figure 2.

## 2.2. Absolute Flux Calibration

The IRAS-60 and AKARI-65 fluxes are, as expected for PNe, roughly linearly correlated. The exact flux-ratio between these two bands depends on the colour temperature at which these sources peak (ie. the slope between 60 and 65  $\mu\text{m}$  changes with dust temperature). In Figure 3 we plot the IRAS-60/AKARI-65 ratio versus AKARI-65 flux (linear y-scale and log x-scale). All PNe (found in both AKARI & IRAS) are plotted in grey, and those with quality-3 data in both bands in black. The correlation between IRAS and AKARI fluxes is much better for the latter “quality” (green) selected set. Sources with black-body temperature 80-100 K peak at wavelengths less than 60  $\mu\text{m}$ , and therefore, as expected, the IRAS-60 fluxes are somewhat higher than the AKARI-65 fluxes. Though based on the SEDs the difference is larger than expected (see below). For the AKARI-90 and IRAS-100  $\mu\text{m}$  the result is similar. In this case we have created a subset from all cross-matches (grey) to include only those targets with quality fluxes and with cirrus emission less than 100 MJy/sr (black). This greatly improves the correlation. See Figure 4.

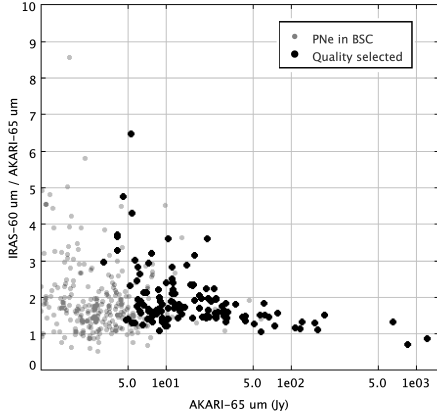


Figure 3. IRAS-60/AKARI-65 flux ratio versus AKARI-65 flux (linear y-scale and log x-scale). Good quality data (quality-3) are those in black.

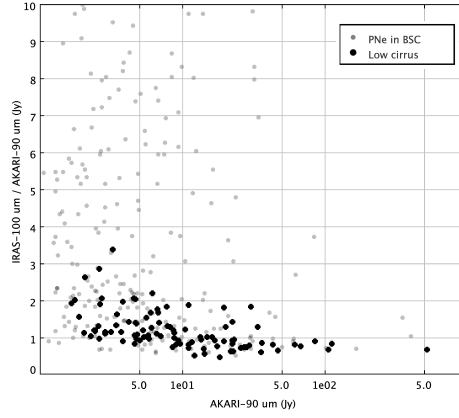


Figure 4. IRAS-100/AKARI-90 flux ratio vs. AKARI-90 flux (linear y-scale and log x-scale). Good quality data and cirrus emission less than 100 MJy/sr are those in black.

### 3. SEDs and Dust Temperatures of the Selected AKARI PNe

There are (only) 14 PNe that are detected in all AKARI/FIS and IRAS bands. We use only these PNe to make a detailed study of the SED. From fitting the AKARI flux data with one-component black-body we find dust temperatures that are systematically lower ( $\sim 25\%$ ) than those derived for the same targets from IRAS fluxes alone. Table 1 list the dust temperatures fitting a single black-body using AKARI data (column 2), and IRAS 12, 25 and  $60 \mu\text{m}$  and AKARI 90 and  $140 \mu\text{m}$  fluxes (column 3). For all 14 PNe the IRAS+AKARI SED is

Table 1. Dust temperatures for PNe detected in all IRAS and AKARI bands.

PN	$T_{\text{AKARI}}$	$T_{12-140}$
A30	46.8	50.0
CRL618	98.0	78.0
PN G009.3+05.7	54.5	61.8
He2-113	60.7	89.0
HE3-1333	52.8	77.4
IC4406	27.0	49.2
M1-78	53.8	66.0
M2-9	42.7	70.9
NGC 3132	30.3	49.0
NGC 6302	45.4	64.0
NGC6369	54.1	70.1
NGC 6572	58.7	97.6
NGC 6720	31.3	53.8
Vo3	27.2	31.8

shown in Figure 5. Also indicated are the cirrus emission values from IRAS. We note that in particular the 65  $\mu\text{m}$  flux seems to be often under-estimated for low-medium ( $<100$  Jy) flux densities and may point to systematic errors in the current  $\beta$  release of the BSC. The difference in the derived  $T_{\text{dust}}$  for both cases arises from taking into account the far-IR 140 and 160  $\mu\text{m}$  fluxes in addition to the more accurate 90  $\mu\text{m}$  flux.

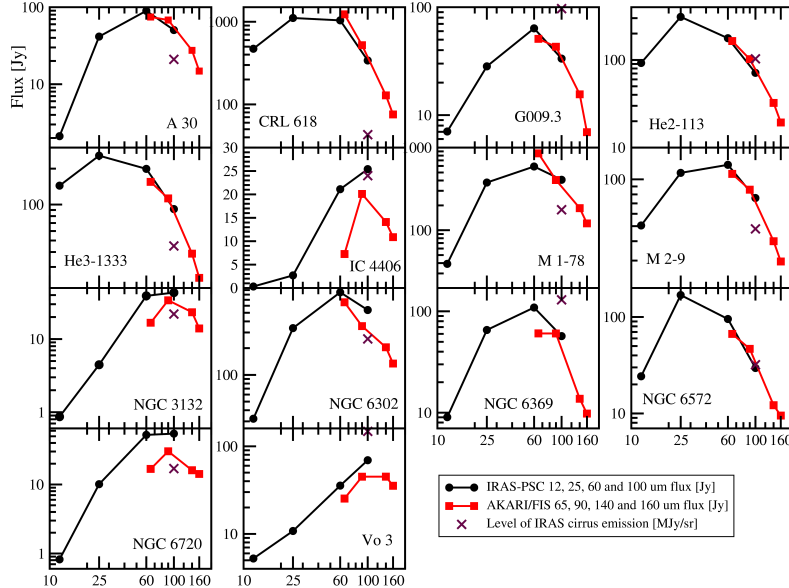


Figure 5. IRAS+AKARI spectral energy distribution of the 14 PNe detected in all bands. The cirrus emission values from IRAS (at 100  $\mu\text{m}$  in MJy/sr) are also indicates (crosses).

#### 4. Summary and Future Work

AKARI performs significantly better than IRAS in the 90/100  $\mu\text{m}$  band. This, in combinations with its further far-infrared coverage, makes it very suitable to detect colder objects (in temperature range from 20 to 70 K). Future work: Several black bodies could be fitted to search for different dust components. AKARI plus IRAS colours could be used to search for new PNe and proto-PNe.

**Acknowledgments.** We thank the organizers for their hospitality and excellent meeting. P.G-L and R.Sz. acknowledge support from the Science Faculty of the European Space Astronomy Center (ESAC). This research is based on observations with AKARI, a JAXA project with the participation of ESA.

#### References

Kerber, F. and Mignani, R. P. and Guglielmetti, F. and Wicenc, A., A&A, 408, 1029